Determination of Surface Energies and Acidity-Basicity Numbers of Protonated and Deprotonated Forms of Poly(sulfonic acid diphenyl aniline) by Inverse Gas Chromatography

Ozlem Yazici, Ferdane Karaman
Department of Chemistry, Yildiz Technical University Davutpasa Campus, 34220 Esenler, Istanbul, Turkey

Protonated form of poly(sulfonic acid diphenyl aniline) (p-PSDA) was synthesized through oxidative chemical polymerization of sodium salt of diphenylamino-4-sulfonic acid in hydrochloric acid and then, its deprotonated form (PSDA) was obtained by neutralization with aqueous ammonium hydroxide solution. The samples were characterized by thermal analysis and Fourier Transform Infrared, Ultraviolet-visible, ^{1}H-NMR spectroscopy techniques. Their dispersive surface energies as well as surface acidity and basicity were determined by inverse gas chromatography at temperatures between 313 and 353 K. The dispersive surface energy of p-PSDA was found to be considerably lower but it increased with temperature while that of PSDA was close to those of conventional polymers and decreased slightly with temperature. According to the Schreiber's procedure, the surfaces of p-PSDA and PSDA were found to be acidic and amphoteric, respectively. It was observed from the electron microscope images p-PSDA chains can form self-organized circular polydisperse micro-sized aggregates in aqueous solutions while PSDA cannot self-organize to form individual aggregates. POLYM. ENG. SCI., 00:000–000, 2015. © 2015 Society of Plastics Engineers

INTRODUCTION

The intrinsically conducting polymers (ICP) have been used in the fields of conducting composites, conducting textiles, rechargeable batteries, corrosion protection of metals, ion exchange membranes, photovoltaics, memory devices, light emitting diodes, sensors actuators, etc. [1, 2]. The conductivity of ICPs can be enhanced through charge carriers by removing or adding electrons into the delocalized π-electrons of the backbone *via* chemical oxidation (p-type doping) or reduction (n-type doping), respectively. Thus, structural defects are created in the conjugated electronic states of the backbone and consequently, geometric parameters such as bond lengths and bond angles change. It is called positive polaron or radical cation when an electron is removed from a polymer chain and consequently a positive charge and an unpaired electron are localized over several repeating units. By removing another electron from the positive polaron, a positive bipolaron or a dication with charge +2 and no spin are localized over several repeating units. Electrical conductivity of oxidized ICPs increase because of extended polymer chains having positive charges on the backbone. Simultaneously, an equal amount of mobile anions with their hydration shells should move into the polymer from chemical environment in order to maintain electroneutrality and consequently, the polymer swells. However, the reduced polymer shrinks because of contraction of the polymer backbone due to the disappearance of positive charge carriers and the simultaneous expelling of the mobile anions out of the polymer. That is why the average thickness of the oxidized films of polyaniline (PANI) and its methoxy derivatives were about 10–30% higher than the reduced ones [3–8]. It was assumed that the appearance of charge carriers through oxidation is accompanied by a local self-ordering of the extended chains into crystalline conducting islands in an amorphous dielectric matrix whereas their disappearance through reduction leads to destruction of the islands [9–11]. In fact, crystalline islands of PANI were experimentally observed as dense inclusions in an amorphous matrix, by means of X-ray structural analysis, luminescence, ellipsometry, electron, and atomic force microscopy [12, 13].

When the counter anions cannot move out of the polymer due to being large or self-doped, i.e., bounded to the polymer, the small mobile cations with their hydration shells are expelled out of the polymer to maintain electroneutrality during oxidation. Because of these opposite effects, the self-doped ICPs cannot considerably swell during oxidation. That is why the change in thickness of self-doped sulfonated polyaniline films between the reduced and oxidized states was found to be negligible (2%) [14]. However, the mechanisms involved are not clear, yet.

The nonconducting emeraldine base form of PANI and its derivatives can be converted into the partly protonated, highly conducting emeraldine salt form simply by treating them with mineral acids [15]. By treatment with acids, protons are added to a fraction of the unprotonated nitrogen atoms. Thus, the number of electrons on the polymer backbone is held constant whereas the number of protons is varied with acid doping. The protonation reaction is reversible. Strictly, on the chain-backbone, PANI acquires positive charges by protonation, however these positive charges are lost by neutralization. The expansion of protonated polymer chains due to positive charges on the backbone and simultaneously, insertion of anions and exclusion of the counter cations must cause change on their surface energies compared to the unprotonated form.

Inverse gas chromatography (IGC) is a promising and reliable technique in determination of surface energies of different solids such as polymer, glass, ceramic, hybrid, blends, etc. [16–19]. The advantage of IGC compared to other methods is

Correspondence to: Ferdane Karaman; e-mail: ferdanekaraman@yahoo.com
Contract grant sponsor: Scientific and Technological Research Projects, TUBITAK; contract grant number: 107T697.
DOI 10.1002/pen.24062
Published online in Wiley Online Library (wileyonlinelibrary.com).
© 2015 Society of Plastics Engineers

that it allows one to study the materials whose surfaces are not smooth, viz. porous, fine powdered or fibrous at a wide temperature range. This technique is based on the retention of different organic probes when they pass through a chromatograph column filled with the solid to be characterized. The retention depends on the attractive forces arising from the differences of their cohesive electron densities between chemical groups on the material surface and probe molecules. The surface energies of solid material in the column are calculated using the free energy of adsorption arising from the retention of probe molecules. The use of nonpolar organic probes such as n-alkanes leads to the determination of dispersive surface free energy while the use of specific organic probes with known acceptor-donor properties leads to specific surface free energy, i.e., acid–base properties.

In this study, it was aimed to investigate the dispersive surface energy and acid–base properties of protonated and deprotonated forms of a sulfonated derivative of PANI, namely, poly(sulfonic acid diphenyl aniline) (PSDA). No study was encountered in the literature concerning the surface energies of sulfonated polyanilines. The results were interpreted by taking into account the conformational changes due to protonation and deprotonation reactions.

EXPERIMENTAL

Materials

Sodium diphenyl amino-4-sulfonate (>99%; Sigma-Aldrich), ammonium persulfate (98%; Sigma-Aldrich), sodium hydroxide (Fluka), sodium sulfate (Merck), hydrochloric acid (37%; Merck), ammonium hydroxide (Sigma-Aldrich), analytical grade ethanol (Merck), tetrahydrofurane (Merck), and diethyl ether (Merck) were used in synthesis of the polymers. The probes n-hexane (Hx), n-heptane (Hp), n-octane (O), n-nonane (N), n-decane (D), dichloromethane (DCM), chloroform (TCM), acetone (Ac), tetrahydrofurane (THF), and ethyl acetate (EA) were supplied from Merck as analytical grades and were used without further purification. The Chromosorb-W (AW-DMCS treated, 80/100 mesh) was also supplied from Merck. Silane-treated glass wool used to plug the ends of the column was obtained from Alltech Associates.

The PSDA protonated with HCl (p-PSDA) was synthesized by oxidative chemical polymerization of sodium diphenyl amino-4-sulfonate with ammonium persulfate at a ratio of [Oxidant]/[Monomer]:1.2 in a medium of 1.2 N HCl at 4°C as described in the literature [20]. The reaction proceeded for 16 h and was ended by addition of ethanol. Dark green precipitate was separated by centrifuge. The precipitate was purified by redispersion in a water/ethanol mixture (1/1) and centrifugation. Bright dark green p-PSDA particles were obtained after drying the precipitate in vacuum at room temperature for 48 h. PSDA was obtained by stirring the p-PSDA in a 15-mL of 1 N ammonium hydroxide solution for 24 h, precipitating with ethanol, purifying in ethanol/water mixture, and drying in vacuum. The color of the acquired PSDA was pale brownish green. It was preferred to synthesize at this lower temperature although there are some procedures conducted at the room temperature [21, 22]. Both of the samples are totally soluble in water but insoluble in the common organic solvents. After their spectroscopic and thermal characterization, dispersive surface energies and acidity–basicity properties were investigated with IGC.

Methods

Characterization of the Samples. Attenuated total reflection-Fourier transform infrared (ATR-FTIR) spectra of the samples were measured using Perkin Elmer Spectrum One FT/IR spectrometer equipped with ATR accessory. Spectral data were collected by contacting the finely ground powder of the samples with the diamond of ATR cell. All spectra were obtained at 2 cm^{-1} resolution after being scanned 60 times. The UV–visible spectra of the samples were recorded using Agilent 8453 UV–Visible spectrophotometer in aqueous solutions. ^{1}H-NMR spectra of the samples were recorded on a Varian Gemini 400 MHz spectrometer using D_2O as solvent. The concentrations of the polymer solution were 15 mg/mL. Differential scanning calorimetric and thermal gravimetric analysis of the samples were measured in nitrogen atmosphere at a heating rate of 10°C/min using TA Instruments SDT Q600. The electron microscope images of the samples were obtained by Philips XL30 ESEM-FEG/EDAX system using STEM (scanning transmission electron microscopy) technique. The samples were prepared by dropping the dilute solution of the polymer in pure water on the copper grids coated with carbon film.

Inverse Gas Chromatography. A typical column preparation is given in the following. The polymer sample was coated on Chromosorb-W in its aqueous solution by stirring rather slowly at 100°C. By means of calcination, the amount of polymers was determined to be approximately 8% on the support material. The coated support material was dried under vacuum at 120°C for 24 h to remove water and then by tapping it was filled into the empty column, which is a stainless steel tubing with 3.2 mm in o.d. and 0.5 m in length made by AlltechAssociates. The column was mounted into the oven of the chromatograph, whose temperature was controlled. A Hewlett–Packard Agilent 6890N Model series II gas chromatograph with a thermal conductivity detector was used to measure the retention time of the probes. Helium was used as carrier gas at a 10 cm^3/min flow rate. The columns were conditioned at 120°C for 24 h under helium before measurements. Trace amounts of probe vapors were injected manually at least in triplicate by a 1-μL Hamilton syringe. The syringe was purged as many times as necessary to attain extreme dilution of the probes. The retention times for each probe on the polymers were measured at temperatures between 313 and 353 K with increments of ten degrees. Studies at higher temperatures were avoided to exclude the contribution coming from bulk absorption of the probe molecules.

THEORY

Dispersive Surface Free Energy

The surface properties of the polymer samples under investigation in the packed columns are determined from the net retention volume, V_N which is directly related to the net retention time of the probe and the flow rate of the carrier gas:

$$V_N = (t_R - t_A) Q \left(\frac{T}{T_f}\right) J \tag{1}$$

where t_R and t_A are the retention times of the probe and the air, respectively, Q is the volumetric flow rate measured at the temperature T_f (K) in the column outlet, T is the column

DOI 10.1002/pen

temperature (K), and J is the James-Martin gas compressibility correction factor [23]. Data from IGC measurements at infinite probe dilution can lead to the determination of the Gibbs free energy of adsorption, ΔG_A, of the probe molecules on the polymer samples by the following equation:

$$\Delta G_A = -RT \ln V_N + C. \quad (2)$$

Here, R is the ideal gas constant and C is a constant depending on the state of adsorption. The Gibbs free energy of adsorption of a polar material has two components: dispersive and specific

$$\Delta G_A = \Delta G_A^D + \Delta G_A^{SP} \quad (3)$$

where the superscripts D and SP refer to dispersive and specific, respectively. The correlation between the Gibbs free energy of desorption, $-\Delta G_A$, and the work adhesion W_A between the probe and the solid material results in the equation:

$$-\Delta G_A = N_A a W_A \quad (4)$$

where N_A is the Avogadro's number, a is the surface area of the probe molecule.

The surface energy, γ, being a combination of nonpolar or dispersive, γ^D, and polar or specific γ^{SP} component is a measure of the free energy on the surface of a material. If a material contains an incohesive electron cloud, the dispersive surface energy tends to be high. Alternatively, a material having polar groups or dipoles on the surface tends to have a high specific surface energy. Specific interactions may be in the form of hydrogen bonding, acid–base, dipole–dipole, charge transfer, electron donor–acceptor complexes, etc. These specific interactions being highly directional and electrostatic are present in addition to the dispersive forces. Fowkes [24, 25] suggested the totality of specific interactions may be treated as Lewis acid–base forces. The thermodynamic work of adhesion between a solid and an adsorbed probe includes only dispersion interactions in the case of nonpolar probes but it includes both dispersive and specific interactions in the case of polar ones. Then, when a nonpolar probe is injected into the carrier gas stream in the chromatograph, it is possible to write:

$$W_A = W_A^D = 2(\gamma_S^D \gamma_L^D)^{1/2} \quad (5)$$

where γ^D denotes the dispersive component of the surface energy, the subscripts S and L indicate the solid and the liquid (i.e., probe), respectively. These relationships were rearranged by Schultz and Lavielle [26] and used to calculate the dispersive surface energy of the solid

$$RT \ln V_N = 2N_A a(\gamma_L^D \gamma_S^D)^{1/2} + C. \quad (6)$$

Thus, for a series of n-alkane probes, a plot of $RT \ln V_N$ against $a(\gamma_L^D)^{1/2}$ will give a linear line, the slope of which is $2N_A(\gamma_S^D)^{1/2}$.

The dispersive component of the surface energy can also be determined by the method given by Dorris and Gray [27].

$$\gamma_S^D = \frac{(-\Delta G_{CH_2})^2}{4N_A^2 . a_{CH_2}^2 . \gamma_{CH_2}} \quad (7)$$

where

$$\Delta G_{CH_2} = -RT \ln \left(\frac{V_N(n+1)}{V_N(n)} \right)$$

Here, ΔG_{CH2} is the slope of the linear line plotted by Gibbs free energy of n-alkanes against their carbon atom number and represents the Gibbs free energy of a single $–CH_2–$ group adsorption and a_{CH2} is the area occupied by a $–CH_2–$ group (0.06 nm^2). γ_{CH_2} is the surface energy of a polymer consisting of only $–CH_2–$ groups given as $\gamma_{CH_2}(mJ/m^2) = 35.6 + 0.058(293 - T)$ where T is the temperature in K.

Acidity and Basicity Constants

The application of IGC to determine the ability of the solid surface to specific interactions is much more difficult than that of dispersive ones since only one chromatographic peak is obtained resulting from both dispersive and specific interactions of a polar probe with a polar solid surface [28]. The term "specific interactions" denotes all types of interactions except dispersive ones. Therefore, specific interactions include the polymer–probe interactions such as acid–base, dipole–dipole, induced dipole–dipole, hydrogen bonding, π-character, and steric effects. Although various scales were proposed in measurement of acidity and basicity of a solid surface, the Gutmann's approach which involves acceptor and donor numbers expressing the ability of the probes to act as electron acceptor and electron donor, respectively, is the most frequently used. The retention volume of the probe acting as electron acceptor, i.e., Lewis acid should be high on the basic polymer surface and low on the acidic polymer surface or vice versa. Ability of the examined surface to the specific interactions is obtained from the specific component of the Gibbs free energy of adsorption, ΔG_A^{SP}. This component is the difference of Gibbs free energies of adsorption between the polar probe, ΔG_A(polar) and a hypothetical n-alkane, ΔG_A(ref), which has the same selected property as the polar probe has.

$$\Delta G_A^{SP} = \Delta G_A(\text{polar}) - \Delta G_A(\text{ref}) = -RT \ln \left(\frac{V_N(\text{polar})}{V_N(\text{ref})} \right). \quad (8)$$

Several authors proposed to select different properties of the probes, e.g., $a(\gamma_L^D)^{1/2}$ by Schultz and Lavielle [26], or vapor pressure by Papirer and Balard [28] or boiling point by Brookman and Sawyer [29]. Then, specific component of the enthalpy of adsorption, H_A^{SP}, is determined from the dependence of ΔG_A^{SP} on temperature:

$$\Delta G_A^{SP} = \Delta H_A^{SP} - T\Delta S_A^{SP} \quad (9)$$

where ΔS_A^{SP} is the specific component of the adsorption entropy of the interaction between the polar probe and the solid surface. By plotting $\Delta G_A^{SP}/T$ as a function of reciprocal of the absolute column temperature, ΔH_A^{SP} can be obtained from the slope of the straight line. However, the estimation of ΔH_A^{SP} might be the largest error source on the obtained acidity and basicity constants.

ΔH_A^{SP} is related to the constants K_A and K_D expressing the ability of the polymer to act as an electron acceptor (acidic) and an electron donor (basic), respectively [30].

$$-\Delta H_A^{SP} = K_A \text{ DN} + K_D \text{ AN}^*. \quad (10)$$

A straight line with the slope of K_A is obtained by plotting $\Delta H_A^{SP}/\text{AN}^*$ against DN/AN* where DN denotes the donor number

TABLE 1. The surface area, a, dispersive surface energy, γ_L^D, Gutmann's donor number, DN, Fowkes's acceptor number, AN*, dielectric constant, ε, and acidic–basic properties of the probes used in this study.

Probes	$a10^{20}$ (m^2)	γ_L^D (mJ/m^2)	DN (kJ/mol)	AN* (kJ/mol)	ε	Acidity/basicity
Hx	51.5	18.4	0	0	1.89	Neutral
Hp	57.0	20.3	0	0	1.92	Neutral
O	62.8	21.3	0	0	1.95	Neutral
N	68.9	22.7	0	0	1.97	Neutral
D	75.0	23.4	0	0	1.99	Neutral
DCM	31.5	27.6	0	16.3	8.93	Acidic
TCM	44.0	25.9	0	22.6	4.81	Acidic
Ac	42.5	16.5	71.2	10.5	20.7	Amphoteric
EA	48.0	19.6	71.6	6.3	8.87	Amphoteric
THF	45.0	22.5	83.7	2.1	7.5	Basic

given by Gutmann and AN* is the acceptor number modified by Fowkes [31]. The values of the constants K_A and K_D calculated in this way are theoretically independent on the column temperature in spite of the fact that some researchers have proposed temperature can change acidic properties of a material [32–34]. Although precise values were given in the literature, relative errors of K_D can be larger because it is determined from the intercept of the straight line. The criterion is that solid material in the column is acidic if the ratio K_A/K_D is higher than 1 whereas it is basic if the ratio is lower than 1. Thus, the solid material should be amphoteric if the ratio is 1.

The characteristics of the probes used in this study were presented in Table 1.

On the other hand, Schreiber et al. [35] have proposed an arbitrary definition for acceptor and donor numbers of the solid material in the column, which are not related to the numbers given by Gutmann. They are defined as follows

$$(AN)_S=(V_N)_{thf}/(V_N)_{ref} \text{ and } (DN)_S=(V_N)_{ch}/(V_N)_{ref} \qquad (11)$$

where $(V_N)_{thf}$, $(V_N)_{ch}$, and $(V_N)_{ref}$ denote the net retention volumes of tetrahydrofurane, chloroform, and n-alkane, respectively, which have the same selected property like boiling point. Similarly to the Gutmann's criterion, solid material in the column is acidic if the ratio $(AN)_S/(DN)_S$ is higher than 1.1 whereas it is basic if the ratio is lower than 0.9. The solid material should be amphoteric if the ratio is between 0.9 and 1.1.

RESULTS AND DISCUSSION

IR Spectra

Figure 1 represents the ATR-FTIR spectra of the samples. The spectrum of p-PSDA exhibits two bands with maxima at 1591 and 1495 cm^{-1} assigned to quinoid and benzenoid ring stretching vibrations, respectively. These bands exhibit a blue-shifting in the spectrum of deprotonated sample, PSDA. Since the ratio of quinoid to benzenoid bands is indicative of the extent of the oxidation state of the polymer, it can be seen both of the samples are approximately half-oxidized, i.e., emeraldine form The band appearing at 1405 cm^{-1} in the PSDA spectrum was attributed to the bending vibrations of inorganic NH_4^+ introduced into the polymer during neutralization. The absence of the peak at 1405 cm^{-1} in the spectrum of p-PSDA exhibits that NH_4^+ cations of ammonium persulfate are excluded from the

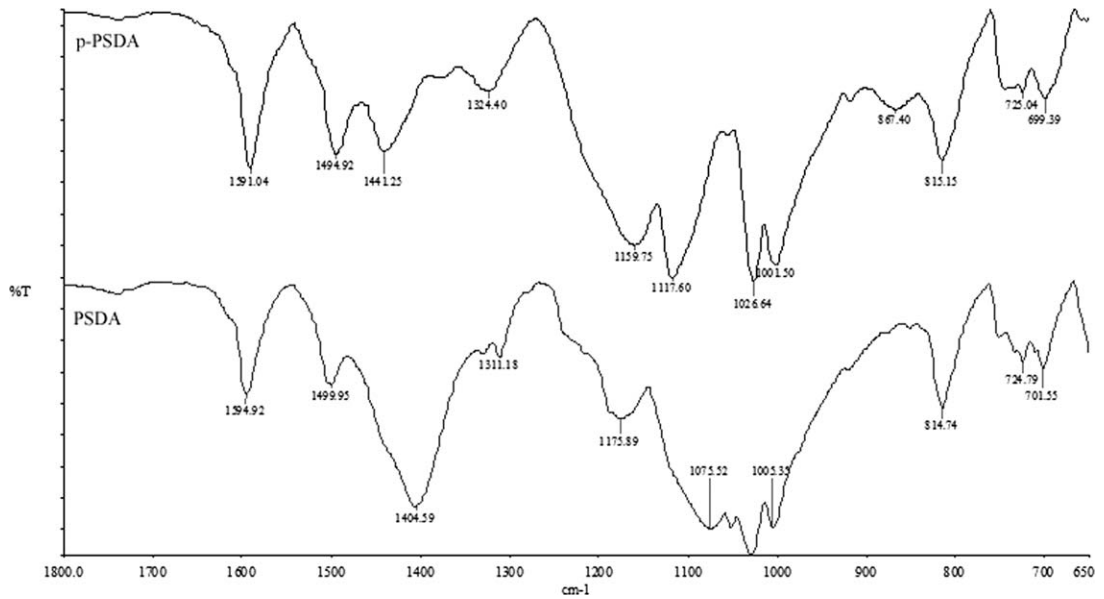


FIG. 1. ATR-FTIR spectra of p-PSDA and PSDA.

 DOI 10.1002/pen

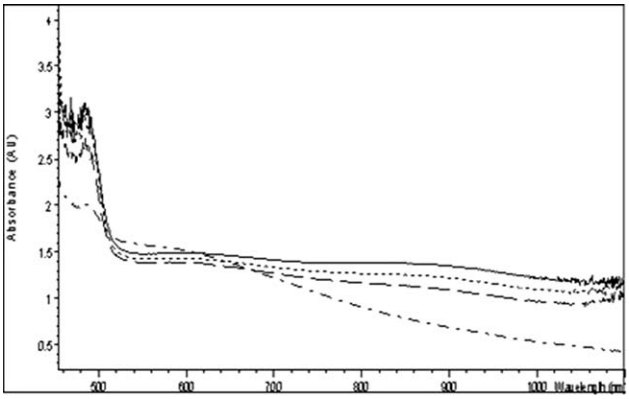


FIG. 2. Conversion of PSDA to p-PSDA with addition of HCl up to pH 3; Lines correspond to the times passing: 0 min. (dashed and dotted), 30 min. (dashed), 45 min. (dotted) and 60 min. (solid) later.

polymer during synthesis to set electroneutrality. This implies p-PSDA bears positive polarons and bipolarons on the backbone. Thus the chains of p-PSDA should be extended because of the repulsive forces between the positive charges on the backbone. The band at 1324 cm^{-1} in the spectrum of p-PSDA corresponds to π-electron delocalization induced by protonation [36]. This band is weaker in the spectrum of PSDA. The peaks at 1118, 1027, and 1002 cm^{-1} in the spectrum of p-PSDA were assigned as symmetric and asymmetric S═O stretching bands of sulfonyl groups [22]. The corresponding peaks in the spectrum of PSDA exhibit a blue shifting. The broad band at 1075 cm^{-1} in the spectrum of PDSA might be attributed to the stretching vibrations of S═O which took part in the self-doping mechanism. It can be concluded from the FTIR-spectra of the polymers p-PSDA should be in an extended conformation but PSDA should be in a more contracted conformation since its vibration bands undergo a blue-shifting probably due to self-doping.

UV–Visible Spectra

The UV–vis. absorption spectra in Fig. 2 are recorded at several time intervals after addition of HCl into the aqueous solution of PSDA to set pH 3. The intensity of the absorption bands of PSDA varies in time as it turns into the p-PSDA by a considerably slow protonation process. The variation in electronic structure of PSDA can be attributed to the change in geometric structure and thus in conformation of the polymer chains by protonation. In the spectrum of PSDA, there are two absorption bands at 490 and 560 nm. The absorption band at 490 nm is assigned to the polaron-π* transition. This assignment is based on the absorption band of polyaniline emeraldine base at 440 nm [37]. The peak position of the polaron-π* transition did not change but its intensity increased considerably by protonation. This suggests the isolated polarons in the PSDA become an ordered polaron lattice in the p-PSDA [38]. The broad bands at ca 560 nm of PSDA and 610 nm of p-PSDA were assigned to the local charge transfer between a negative charge centered on the quinoid ring and the positive charge centered on the benzenoid rings (charge transfer exciton). This assignment is based on the absorption band of sulfonated polyaniline at 620 nm [39]. It can be stated the loss of planarity of PSDA chains decreases the conjugation of the polymer chains, thus the exciton transition shifts to lower wavelength region, however increasing stiffness of the chain by protonation increases the conjugation of the polymer, thus the transition shifts to higher wave lengths in the p-PSDA. The delocalized band beyond 750 nm, called free carrier tail, in the spectrum of p-PSDA was attributed to the intraband transitions within the half-filled polaron band [37]. It can be concluded from the UV–vis. spectra the polaronic moieties are isolated inside the contracted chains of PSDA because of self-doping interaction between pendant sulfonyl group and positive charges on the nitrogen atoms while an ordered polaron lattice exists on the more extended chains of p-PSDA. In other words, in Fig. 2, externally doped state is recovered by protonation as the smaller HCl molecules replace the pendant sulfonic acid units. Therefore, it can be stated p-PSDA is an externally doped but PSDA is a self-doped forms of the polymer.

^{1}H-NMR Spectra

The proton NMR spectra of the sodium diphenyl amino-4-sulfonate monomer, p-PSDA and PSDA are presented in Fig. 3. The solutions of the NMR samples were prepared at the same concentration (15 mg/mL) and they were transparent in D_2O during measurements. In the spectrum of monomer, two doublets at 6.9 and 7.5 ppm were assigned to the aromatic protons of phenyl sulfonate group while the doublet at 6.8 ppm and the triplet at 7.2 ppm were assigned to the aromatic protons of phenyl group. The spectrum of p-PSDA shows two weak doublets of the aromatic protons of pendant phenyl sulfonic acid group at higher ppm values. It is evident the aromatic protons of the backbone cannot be solvated by the D_2O. The spectrum of PSDA shows only a broad signal due to the aromatic protons between 6 and 8.8 ppm. This indicates the aromatic protons of PSDA cannot at all be solvated by D_2O because of self-doping. The ^{1}HNMR spectra suggest p-PSDA has a more extended conformation compared to PSDA.

Thermal Analysis

As can be seen from differential scanning calorimetric and thermogravimetric analysis in Fig. 4, p-PSDA has no thermal transition temperature and it was thermally stable up to decomposing temperature at 225°C. The absence of a glass transition suggests that p-PSDA has no amorphous fraction and decomposes before melting.

Dispersive Surface Free Energy

The dispersive surface energies of the samples in Table 2 were determined by the methods proposed by Schultz and Lavielle from the plot of $RT\ \ln V_N$ versus $a\sqrt{\gamma_L^D}$ as well as by the method proposed by Dorris and Gray from the plot of $RT\ \ln V_N$ versus number of carbon atoms in the n-alkane series using *Eqs. 6* and *7*, respectively, as a function of temperature. All of these plots represented good linear variations.

The dispersive surface energy of PSDA was found very close to those of conventional polymers such as polyethylene, polypropylene, polystyrene, poly(methyl methacrylate) [40] whereas that of p-PSDA was found lower around ambient conditions but increased with temperature. The low dispersive surface energy of p-PSDA should be reasonable since it is expected lower electron cloud density from the extended conformations. The

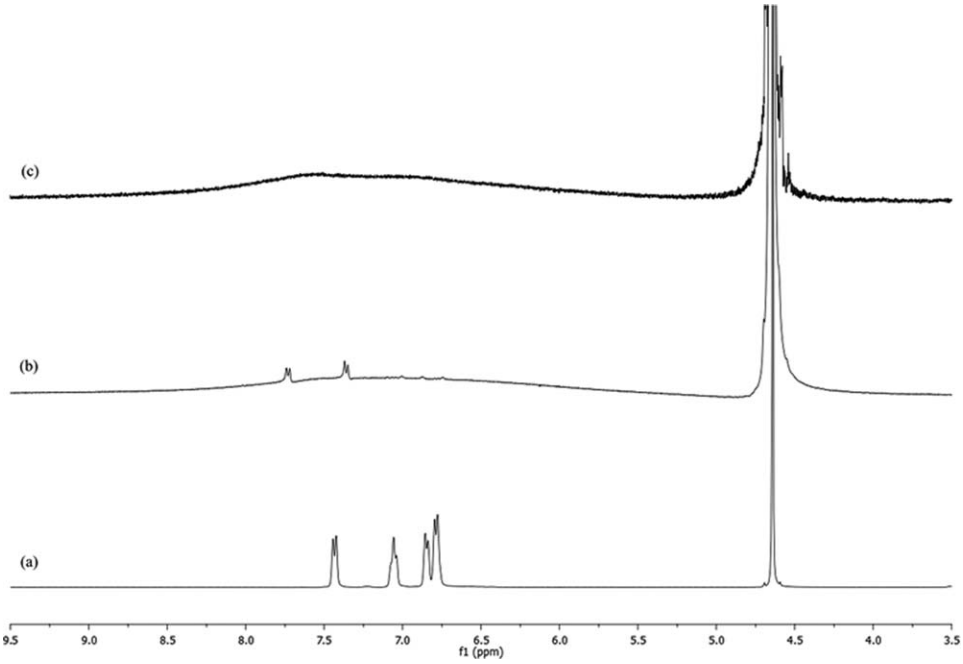


FIG. 3. ^{1}H-NMR spectra of monomer (a), p-PSDA (b) and PSDA (c) in D_2O.

increase in dispersive surface energy of p-PSDA with temperature can be explained by decreasing repulsive forces between polarons/bipolarons due to increasing thermal motions with temperature.

By IGC, considerably higher dispersive surface energies were determined for conducting polymers in the literature. Compared to the dispersive surface energy of PANI protonated with HCl in the literature [41–47], dispersive surface energies of both samples in the present study were lower. This can be attributed to the electron withdrawing effect of the pendant sulfonyl group on the polymers in the present study. No study was found in the literature related to the dispersive surface energies of sulfonated conducting polymers. Dispersive surface energy of emeraldine base of PANI which is a deprotonated form increased with temperature from 29 mJ/m^2 at 140°C to 94 mJ/m^2 at 170°C. However, the dispersive surface energy of PANI protonated with ethyl benzene sulfonic acid decreased with temperature from 150 mJ/m^2 at 80°C to 74 mJ/m^2 at 130°C [41] while that of PANI protonated with HCl slightly decreased with temperature from 89 mJ/m^2 at 58°C to 87 mJ/m^2 at 68°C [42, 43]. It can be stated from these literature data the dispersive surface energy of protonated PANIs increases with the size of the counter anion since the dispersive surface energy of PANI protonated with ethyl benzene sulfonic acid (150 mJ/m^2) is higher than that of PANI protonated with HCl (87 mJ/m^2) at temperatures around 74°C. On the other hand, the magnitude of dispersive surface energy of conducting polypyrrole was found to be 42, 61, and 106 mJ/m^2 if the counter anions are Cl^-, NO_3^-, and $Fe(CN)_6^{4-}$, respectively [44–47]. By taking into account the dielectric constants of HCl, HNO_3, and HCN which are 5, 19, and 115, respectively, it can be stated dispersive surface energy of an ICP is directly proportional to the magnitude of electrical polarization of the counter anions. It is obvious the dielectric constant of the dopant anion considerably affects dispersive surface energy of polypyrrole in the IGC measurements. Thus, it can be obtained meaningful information in comparison of the dispersive surface energies of the doped ICPs if the dielectric constants of the counter ions are close to each other. Since the dielectric constants of NH_4Cl (ε:7) and HCl (ε:5) are close, the comparison of the dispersive surface energies of p-PSDA including chloride dopant anions and PSDA having ammonium cations can give

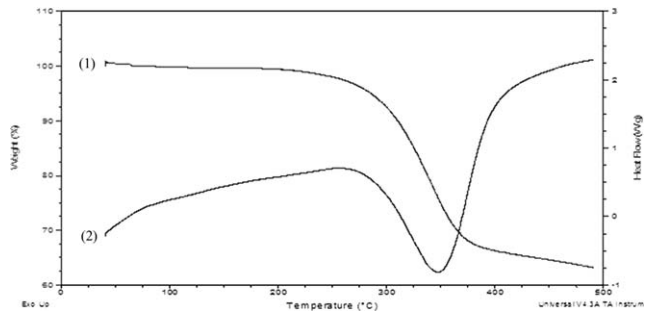


FIG. 4. TGA (1) and DSC (2) traces of p-PSDA.

TABLE 2. Dispersive surface energies, γ_S^D of p-PSDA and PSDA samples.

	p-PSDA		PSDA	
T (K)	S-L	D-G	S-L	D-G
γ_S^D (mJ/m^2)				
313	15	14	37	38
323	17	17	34	36
333	22	23	34	36
343	31	32	31	33
353	42	44	27	30

S-L: Schultz and Lavielle [26].
D-G: Dorris and Gray [27].

DOI 10.1002/pen

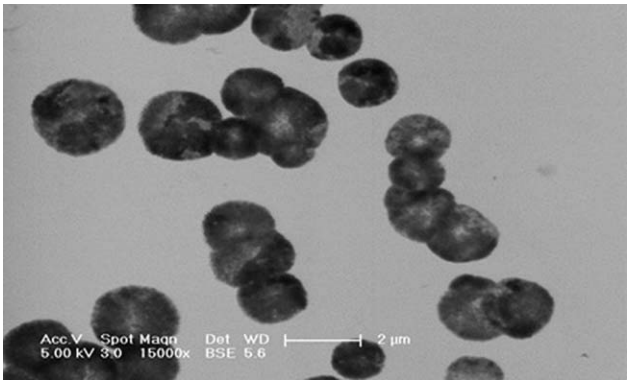


FIG. 5. STEM image of p-PSDA in aqueous solution.

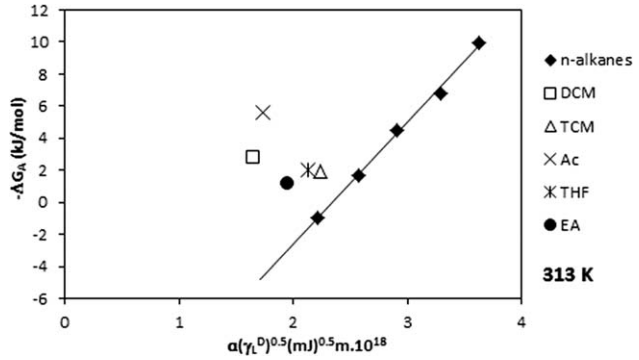


FIG. 7. The variation in Gibbs free energy of adsorption with the term $a\sqrt{\gamma_L^D}$ of the probes for PSDA.

meaningful information related to their chain conformations. Thus, it can be stated from the IGC data in the present study the chains of p-PSDA has a more extended conformation than those of PSDA since dispersive surface energy of p-PSDA is lower.

It was reported the average thickness of oxidized PANI films were about 10–30% higher than that of the reduced form due to a swelling process caused by water/anion insertion [3–8]. The mechanisms responsible for swelling of oxidized PANI is the expansion of polymer chain because of repulsive forces between positive charges on half of the nitrogen atoms and the insertion of anions and water molecules from the solution into the bulk polymer in order to maintain electroneutrality of the polymer. In case of p-PSDA, all of the pendant sulfonyl groups are protonated, i.e., neutral and half of the nitrogen atoms in the backbone are positively charged. Therefore, the net charge of p-PSDA chains should be positive and consequently be in an extended conformation because of repulsion between the positive charges. Some chloride anions with their hydration shells might have migrated from environment into the p-PSDA to maintain electroneutrality. However, in case of PSDA, all of the pendant sulfonyl groups should be negatively charged. A half of these negatively charged pendant sulfonyl groups are neutralized by the positively charged nitrogen atoms on the backbone, that is, PSDA is self-doped. Concurrently, some ammonium cations with their hydration shells should have moved from solution into the polymer bulk in order to neutralize another half of the pendant sulfonyl groups of PSDA. In fact, the FTIR spectrum

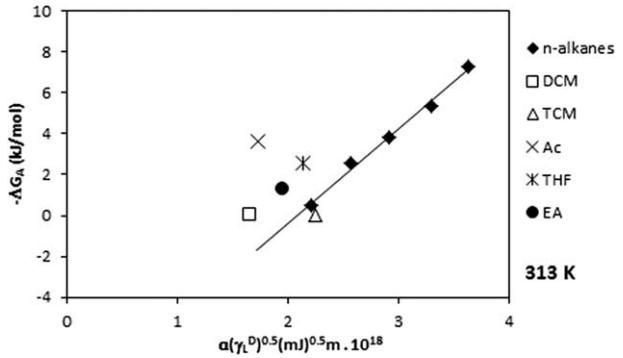


FIG. 6. The variation in Gibbs free energy of adsorption with the term $a\sqrt{\gamma_L^D}$ of the probes for p-PSDA.

indicates the presence of ammonium group in the PSDA (Fig. 1). Dispersed heterogeneous individual circular aggregates in STEM image of the p-PSDA in Fig. 5 can be attributed to the self-organized aggregations of the extended chains. No self-organized individual aggregates were observed in the case of PSDA probably because of self-doping. Thus, it can be stated the morphology of p-PSDA in Fig. 5 confirms its low dispersive surface energy at low temperatures.

Acidity and Basicity Constants

In this study, the specific component of the Gibbs free energy of adsorption, ΔG_A^{SP} of the polar probe on polymer was estimated using three physical properties, i.e., the term $a\sqrt{\gamma_L^D}$, logarithm of saturated vapor pressure and boiling point according to Eq. *8*. The plots which the term $a\sqrt{\gamma_L^D}$ was used as the abscissa were depicted in Figs. 6 and 7 as an example for p-PSDA and PSDA, respectively. It is clear from the figures the acidic probe, TCM, is adsorbed on the surface of PSDA but it is not adsorbed on the surface of p-PSDA. However, another acidic probe, DCM, is adsorbed on the surface of p-PSDA as much as the basic probe, THF. This situation can be explained with the difference of their dielectric constants given in Table 3. The dielectric constant of DCM is two times higher than that of TCM. A high dielectric constant can generate dipole–dipole and induced dipole–dipole interactions and consequently self-association between probe molecules in the column in spite of being in trace amount. As seen in the figures, adsorption free energy of the amphoteric probe, Ac, is also higher than that of the basic one, THF, on p-PSDA probably because of self-association since it has higher dielectric constant than THF. It is also emphasized in the literature the self-association of polar probes plays an important role in the retention process [44].

The specific components of the enthalpies of adsorption ΔH_A^{SP} of the probes were calculated from the slopes of the linear

TABLE 3. The constants of acidity, K_A and basicity, K_D of p-PSDA and PSDA determined by *Eq. 10* at temperatures between 313 and 353 K.

	K_A			K_D			K_A/K_D		
	$a(\gamma)^{1/2}$	ln p	T_b	$a(\gamma)^{1/2}$	ln p	T_b	$a(\gamma)^{1/2}$	ln p	T_b
p-PSDA	0.038	0.21	0.22	0.033	0.20	0.19	1.15	1.05	1.16
PSDA	0.11	0.088	0.10	0.38	0.11	0.13	0.29	0.80	0.77

TABLE 4. The numbers of acidity, $(AN)_S$ and basicity, $(DN)_S$ of p-PSDA and PSDA determined from *Eq. 11*.

	$(AN)_S$			$(DN)_S$			$(AN)_S/(DN)_S$		
T (K)	$a(\gamma)^{1/2}$	ln p	T_b	$a(\gamma)^{1/2}$	ln p	T_b	$a(\gamma)^{1/2}$	ln p	T_b
p-PSDA									
313	2.4	2.2	2.3	0.77	0.92	1.0	3.1	2.4	2.3
323	2.1	1.9	2.0	0.63	0.77	0.85	3.3	2.5	2.4
333	1.6	1.4	1.5	0.68	0.85	0.94	2.3	1.7	1.6
343	2.6	2.4	2.5	0.75	0.98	1.1	3.5	2.4	2.3
353	1.8	1.7	1.7	0.68	0.92	1.0	2.7	1.8	1.7
PSDA									
313	3.7	3.2	3.5	2.4	3.3	3.8	1.5	1.0	0.9
323	3.1	2.7	2.9	2.3	3.1	3.5	1.3	0.9	0.9
333	3.0	2.7	2.9	1.9	2.5	2.8	1.6	1.1	1.0
343	2.8	2.6	2.7	1.5	2.0	2.2	1.8	1.3	1.2
353	2.3	2.2	2.2	1.3	1.7	1.8	1.8	1.3	1.2

lines of $\Delta G_A^{SP}/T$ against $1/T$ according to *Eq. 9*. The constants of acidity, K_A and basicity, K_D of the polymers were obtained by using *Eq. 10* and they were collated in Table 3.

The magnitudes of K_A/K_D in case of p-PSDA are close to 1 while those of PSDA are lower especially if the term $a\sqrt{\gamma_L^D}$ is used as the abscissa. This means p-PSDA is almost amphoteric but PSDA is basic according to Gutmann's approach. It is obvious in Fig. 6 the acidic probe, TCM, does not exhibit a specific interaction with p-PSDA since it has a lower adsorption Gibbs free energy than the corresponding n-alkane. This indicates p-PSDA has no basic sites on its surface. On the other hand, in Fig. 7, the closeness of adsorption Gibbs free energy of acidic TCM and basic THF suggests that PSDA has amphoteric character. Thus, it can be stated the constants denoting acidity and basicity obtained with Gutmann's approach in Table 4 are only approximate values, at least in this study. In fact, pH measurements clearly show the aqueous solution of p-PSDA is more acidic than that of PSDA, viz. pH 3.01 for the former and pH 5.90 for the latter. Thus, p-PSDA should be acidic.

The numbers of acidity $(AN)_S$ and basicity $(DN)_S$ of the polymers that are not related to the constants, K_A and K_D were also calculated according to Schreiber's procedure as given in *Eq. 11* and the results were collated in Table 4. The $(V_N)_{ref}$ values were estimated from the logarithm of net retention volume of the hypothetic n-alkane with the same physical property which the polar probe has. The ratios of acidity number to basicity number in Table 4 suggest p-PSDA is acidic whereas PSDA is amphoteric especially if the boiling point is selected as the abscissa. This result is in agreement with the pH measurements in their aqueous solutions. In addition, it is reasonable to obtain the p-PSDA as acidic since its FTIR and UV–vis. spectra suggest it has positive polarons/bipolarons and consequently it should be a Lewis acid. It is also reasonable to obtain the PSDA as amphoteric since it has both positively charged nitrogen atoms in the backbone and negatively signed pendant sulfonyl ions. Therefore, the Schreiber's approach seems more reasonable than the Gutmann's approach in the determination of acidity and basicity at least in this study. On the other hand, it seems the logarithm of vapor pressure or the boiling point that is easily reached in literature can be used more accurately than the term $a\sqrt{\gamma_L^D}$ as the physical property of the probes in the abscissa.

CONCLUSION

The following conclusions were reached from the results obtained in this study:

1. It was revealed PSDA is a self-doped form while p-PSDA is an externally doped form.
2. Using IGC, the dispersive surface energy of the p-PSDA was found lower than that of conventional polymers since it has extended conformation resulting from the repulsive forces between positive polarons/bipolarons at temperatures close to the ambient conditions.
3. The dispersive surface energy of PSDA was found close to the conventional polymers and slightly decreased with temperature.
4. The circular microsized self-organized individual aggregates observed on the STEM images in the aqueous solution of p-PSDA were attributed to its extended chains due to repulsive forces between the positive polarons/bipolarons.
5. This study suggests IGC might be used to obtain quantitative information related to the conformational changes occurring by doping, at least in this study.
6. p-PSDA was found almost amphoteric while PSDA was basic according to the Gutmann's approach; however, p-PSDA was found acidic while PSDA was amphoteric according to the Schreiber's approach. This suggests Schreiber's approach is more reasonable compared to Gutmann's approach.

ACKNOWLEDGEMENTS

One of the authors wishes to thank for her fellowship (No: 2211) to the Scientists Support Department, BIDEB-TUBITAK, partly by Scientific Research Project Coordinates. The authors would like to thanks to Assoc. Prof. Dr. Dolunay Sakar and Assist. Prof. Dr. Fatih Cakar (Department of Chemistry, Yildiz Technical University) for their technical supports in synthesis.

REFERENCES

1. T.A. Skotheim, R.L. Elsenbaumer, and J.R. Reynolds, *Handbook of Conducting Polymers*, 2nd ed., Marcel Dekker, New York (1998).
2. K.M. Ziadan, in: *Conducting Polymers Application in New Polymers for Special Applications*, Vol. **1**, A.S. Gomes, Ed., InTech Open Access Pub., Rijeka, Croatia, 3 (2012).
3. C.M.G.S. Cruz and E.A. Ticianelli, *J. Electroanal. Chem.* **428**, 185 (1997).
4. M. Kaneko and K. Kaneto, *React. Funct. Polym.*, **37**, 155 (1998).
5. M. Kaneko and K. Kaneto, *Synth. Met.*, **102**, 1350 (1999).
6. M. Kaneko and K. Kaneto, *Polym. J.*, **33**, 104 (2001).
7. M. Kaneko and K. Kaneto, *Appl. Biochem. Biotech.*, **96**, 13 (2001).
8. L. Lizarraga, E.M. Andrade, and F.V. Molina, *J. Electroanal. Chem.*, **561**, 127 (2004).
9. A.J. Epstein, J. Joo, R.S. Kohlman, G. Du, A.G. MacDiarmid, E.J. Oh, Y. Min, J. Tsukamoto, H. Kaneko, and J.P. Pouget, *Synth. Met.*, **65**, 149 (1994).
10. A.B. Kaiser, *Adv. Mater.*, **13**, 927 (2001).
11. I.Y. Sapurina and M.A. Shishov, in: *Oxidative polymerization of Aniline: Molecular Synthesis of Polyaniline and Formation*

 DOI 10.1002/pen

of Supramolecular Structures in New Polymers for Special Applications, *Vol. 9*, A.S. Gomes, Ed., InTech Open Access Pub., Rijeka, Croatia **251** (2012).

12. F.L. Leite, W.F. Alves, M. Mir, Y.P. Mascarenhas, P.S.P. Herrmann, L.H.C. Mattoso, and O.N. Oliveira, *Appl. Phys. A Mater. Sci. Process.*, **93**, 537 (2008).
13. F. Lux, G. Hinrichsen, and M.M. Pohl, *J. Polym. Sci. B: Polym. Phys.*, **32**, 1957 (2003).
14. R.M.Q. Mello, R.M. Torresi, S.I.C. Torresi, and E.A. Ticianelli, *Langmuir*, **16**, 7835 (2000).
15. A.G. MacDiarmid, *Angew. Chem. Int. Ed.*, **40**, 2581 (2001) and A.G. MacDiarmid, J.C. Chiang, A.F. Richter, and A.J. Epstein, Synth. Met., 18, 285 (1987).
16. A. Voelkel, *Chemometr. Intell. Lab.*, **72**, 205 (2004).
17. A. Voelkel, K. Milczewska, and K. Heberger, *Anal. Chim. Acta*, **559**, 221 (2006).
18. A. Voelkel, B. Strzemiecka, K. Adamska, and K. Milczewska, *J. Chromatogr. A*, **1216**, 1551 (2009).
19. A.S. Reddy, P.R. Rani, and K.S. Reddy, *Polym. Eng. Sci.*, **53**, 1780 (2013).
20. F. Hua and E. Ruckenstein, *J. Polym. Sci. A*, **42**, 2179 (2004).
21. C. DeArmitt, S.P. Armes, J. Winter, F.A. Uribe, S. Gottesfeld, and C.A. Mombourquette, *Polymer*, **34**, 158, (1993).
22. M.T. Nguyen, P. Kasai, J.L. Miller, and A.F. Diaz, *Macromolecules*, **27**, 3625 (1994).
23. J.M.R.C.A. Santos and J.T. Guthrie, *Mater. Sci. Eng. R*, **50**, 79 (2005).
24. F.M. Fowkes, *J. Adhes.*, **4**, 155 (1972).
25. F.M. Fowkes, *J. Adhes. Sci. Technol.*, **1**, 7 (1987).
26. J. Schultz and L. Lavielle, *Polymer Surface and Interfaces*, *Vol. 2*, Chichester, Wiley (1993).
27. G.M. Dorris and D.G. Gray, *J. Colloid Interface Sci.*, **77**, 353 (1980).
28. E. Papirer and H. Balard, in: *Interfacial Phenomena in Chromatography*, E. Pefferkorn, Ed., Marcel Dekker, New York, 145 (1999).
29. D. Brookman and D. Sawyer, *Anal. Chem.*, **4**, 106 (1968).
30. V. Gutmann, *TheDonor–Acceptor Approach to Molecular Interactions*, Plenum Press, New York (1978).
31. F.L. Riddle and F.M. Fowkes, *J. Am. Chem. Soc.*, **112**, 3259 (1990).
32. D. Cava, R. Gavara, J.M. Lagarón, and A. Voelkel, *J. Chromatogr. A*, **1148**, 86 (2007).
33. H. Grajek, J. Paciura-Zadrozna, and Z. Witkiewicz, *J. Chromatogr. A*, **1217**, 3116 (2010).
34. A. Voelkel, *Crit. Rev. Anal. Chem.*, **22**, 411 (1991).
35. H.P. Schreiber, J.M. Viau, A.Fetoui, and Z. Deng, *Polym. Eng. Sci.*, **30**, 263 (1990).
36. Z. Ping, *J. Chem. Soc. Faraday Trans.*, **92**, 3063 (1996).
37. Y. Xia, J.M. Wiesinger, A.G. MacDiarmid, and A.J. Epstein, *Chem. Mater.*, **7**, 443 (1995).
38. A.J. Epstein, J.M. Ginder, F. Zuo, R.W. Bigelow, H.S. Woo, D.B. Tanner, A.F. Richter, W.S. Huang, and A.G. MacDiarmid, *Synth. Met.*, **18**, 303 (1987).
39. J. Yue, Z.H. Wang, K.R. Cromack, A.J. Epstein and A.G. MacDiarmid, *J. Am. Chem. Soc.*, **113**, 2665 (1991).
40. Solid surface energy data (SFE) for common polymers. http://www.surface-tension.de/solid-surface-energy.htm. Accessed January 23, 2014.
41. A. Al-Ghamdi and Z.Y. Al-Saigh, *J. Chromatogr. A*, **969**, 229 (2002).
42. M.M. Chehimi, M.L. Abel, Z. Sahraoui, K. Fraoua, S.F. Lascelles, and S.P. Armes, *Int. J. Adhes. Adhes.*, **17**, 1 (1997).
43. M.M. Chehimi, M.L. Abel, C. Perruchot, M. Delamar, S.F. Lascelles, and S.P. Armes, *Synth. Met.*, **104**, 51 (1999).
44. E. Pigois-Landureau and M.M. Chehimi, *J. Appl. Polym. Sci.*, **49**, 183 (1993).
45. M.M. Chehimi, S.Lascelles, and S.P. Armes, *Chromatographia*, **41**, 671 (1995).
46. M.M. Chehimi, M.L. Abel, E. Pigois-Landureau, and M. Delamar, *Synth. Met.*, **60**, 183 (1993).
47. M.M. Chehimi, E. Pigois-Landureau, and M.M. Delamar, *J. Chim. Phys.*, **89**, 1173 (1992).